Using Optimisation Techniques within a Rapid Distortion Theory Framework to Improve Trailing Edge Noise Predictions

Sarah Stirrat[1], Mohammed Afsar[1], Edmondo Minisci[1] and Ioannis Kokkinakis[1]
[1] Department of Mechanical & Aerospace Engineering, University of Strathclyde
75 Montrose St, Glasgow, G1 1XJ, United Kingdom

ABSTRACT

Goldstein, Leib & Afsar [1] found that the acoustic spectrum for the round jet scattering problem is given a formula that involves the Fourier transform of the turbulence function, R_{22}. We extend this acoustic model to enable representation of the anti-correlation region which was previously excluded. There are several parameters within the model which need to be selected in order to find the optimum acoustic spectrum across acoustic Mach number and far-field angle. Here we discuss the optimisation methods which were used to obtain these parameters.

1. Introduction

The canonical problem of a jet flow interacting with a plate positioned parallel to the level curves of the streamwise mean flow has received much attention in Aero-acoustics research community as a representation of jet installation effects. Rapid-distortion theory (RDT) involves relating an upstream convected quantity that serves as the problem input to measureable turbulence and then determine the far field radiated sound, as the response to this. Goldstein, Leib & Afsar (GLA19) [1] find that the acoustic spectrum for the round jet scattering problem is given by (Eqs. 6.26 & 6.27 in their paper):

$$I(\boldsymbol{x},\omega) \rightarrow (\rho_\infty c_\infty^2)^2 \int_{-\infty}^{0}\int_{-\infty}^{0} D(u,\tilde{u};\theta)\bar{S}(u,\tilde{u};k_3^*,\omega)\,du\,d\tilde{u}, \tag{1}$$

where $D(u,\tilde{u};\theta)$ is the round jet directivity factor determined by application of the Wiener-Hopf technique (i.e. Eq. 13 in Afsar *et al* [2]) and,

$$\bar{S}(u,\tilde{u};k_3^*,\omega) = \int_{-\infty}^{0}\int_{-\infty}^{0} S(u,\tilde{u}|v,\tilde{v};k_3^*,\omega)\left|\frac{dz}{dW}\right|^2\left|\frac{d\tilde{z}}{d\tilde{W}}\right|^2 dv\,d\tilde{v}, \tag{2}$$

GLA19 showed that the function $S(u,\tilde{u}|v,\tilde{v};k_3^*,\omega)$ is defined by

$$S(u,\tilde{u}|v,\tilde{v};k_3^*,\omega) = \left[\frac{dU/du}{U^2(u)}\frac{dU/d\tilde{u}}{U^2(\tilde{u})}\nabla u\tilde{\nabla}\tilde{u}\omega^2\right]F(u,\tilde{u},v,\tilde{v}) \tag{3}$$

This result shows, among other things, that $S(u,\tilde{u}|v,\tilde{v};k_3^*,\omega)$ is directly proportional to the Fourier transform of the streamwise-independent transverse velocity correlation function, R_{22} (see Afsar *et al* [2]).

We allow the spectral function $F(u,\tilde{u},v,\tilde{v})$ to be more general than that used in GLA19 (Eq. 4.22 in their paper) by including anti-correlation effects. Hence, in this case, $F(u,\tilde{u},v,\tilde{v})$ is given by the following:

$$F(u,\tilde{u},v,\tilde{v}) = l_2^4 A(u,\tilde{u}) \Bigg[(1-a_1)\frac{\tau_0 f}{\pi\sqrt{1+\tilde{\omega}^2}}K_1(f\sqrt{1+\tilde{\omega}^2}) + \frac{a_1\tau_0 f^2\tilde{\omega}^2}{\pi(1+\tilde{\omega}^2)} \left[\frac{1}{2}(K_0(f\sqrt{1+\tilde{\omega}^2}) + K_2(f\sqrt{1+\tilde{\omega}^2})) + \frac{K_1(f\sqrt{1+\tilde{\omega}^2})}{f\sqrt{1+\tilde{\omega}^2}}\right]\Bigg] \tag{4}$$

Where K_0, K_1, and K_2 are the modified Bessel functions of the second kind of order $0, 1$, and 2 respectively, $A(u,\tilde{u})$ is the amplitude function and f is the space-time decay function.

This form of $F(u,\tilde{u},v,\tilde{v})$ was derived by including the next term in the power series expansion of R_{22} that is of the form $1 - a_1\hat{\tau}\partial/\partial\hat{\tau}$, which acts upon the exponentially decaying de-correlation function given by (B.5) in GLA19, where the "time delay" now includes additional convective effects in coordinates (y_1, u) and $(\tilde{y}_1, \tilde{u})$ respectively.

The upshot of using Eq. 4 as the form of $F(u,\tilde{u},v,\tilde{v})$ is the introduction of an additional parameter (a_1) to the acoustic spectrum. So, there are several parameters within the model (a_1, l_2, l_3, τ_0) which need to be selected in order to find the optimum acoustic spectrum predictions across acoustic Mach number and far-field angle, while also representing the turbulence structure. In the following sections we discuss the different optimisation methods which were used to obtain these parameters.

2. Optimisation Methods

There are various approaches to determine the parameters in $F(u,\tilde{u},v,\tilde{v})$. One way is by hand as in GLA19, but here we use the following methods:

Method 1: Optimise the acoustic model to find the 4 parameters.

Method 2: Optimise the R_{22} model to find a_1, and hand-tune the other 3 parameters for acoustic predictions.

Method 3: Optimise the R_{22} model to find a_1, and optimise the acoustic model to find the other 3 parameters.

Corresponding author: Second Author
E-mail address: mohammed.afsar@strath.ac.uk

All methods were performed using the multi-population adaptive inflationary differential evolution algorithm (*MP-AIDEA*) which is based on differential evolution and is fully described in Di Carlo et al [3].

3. Comparison of Methods 1,2, and 3 for Trailing Edge Noise Predictions

Method 1 was used to find the four parameters through optimisation of our acoustic model against the experimental data in GLA19. The acoustic prediction is shown in Figure. 1 in green. We can see that it matches the data well. However, the turbulence correlation function R_{22} that we use is a function of a_1: $R_{22} \sim (1-a_1\tau)e^{-\tau}$ and the value for a_1 that was found from this method does not give a good representation of R_{22}, as shown in Figure. 2. There is no anti-correlation region and the initial decay is too slow. Note, that we've allowed $\tau U_c/D \to 10$ to show where the model goes to zero, there is no turbulence data at these locations most likely due to measurement difficulties.

Hence, for methods 2 and 3, we optimise the R_{22} model separately against experimental data from Bridges [4]. This means that the anti-correlation region is represented and the initial decay is steeper, as shown in Figure. 2 in black. Only the initial de-correlation is of interest, therefore we have used a simple model for R_{22}. A different model could be used to capture the oscillations but this would make the acoustic model much more complicated and have no improvement on the acoustic spectrum predictions.

In method 2, we use this value ($a_1 = 0.84842$) in the acoustic model and hand tune the other parameters to find the best prediction. We aimed to find one set of parameters for all acoustic Mach numbers. However, it was found that due to the level shift in the acoustic spectrum, one parameter (l_2) must change for each Mach number. The acoustic prediction for this is shown in Figure. 1 in red and is similar to the first method. However, hand tuning these parameters is not ideal as it relies on human judgement as to what is a 'good' prediction.

Hence, for method 3 we use the same a_1 (0.84842) and then optimise our acoustic model to find the other three parameters. This allows us to find the optimum predictions for the acoustic spectrum while also having a good representation of the turbulence structure. This prediction is shown in Figure. 1 in black. Again, we see that the prediction is similar to the methods 1 and 2.

The parameters for each method are shown in Table. 1.

Table 1 Ma=0.9 $\theta = 90$: Comparison of parameters found from the optimisation methods

Method	l_2	l_3	τ_0	a_1
1	0.83746	3.0393	4.4323	0.40154
2	0.55	5.0	5.0	0.84842
3	0.59905	2.7	5.3207	0.84842

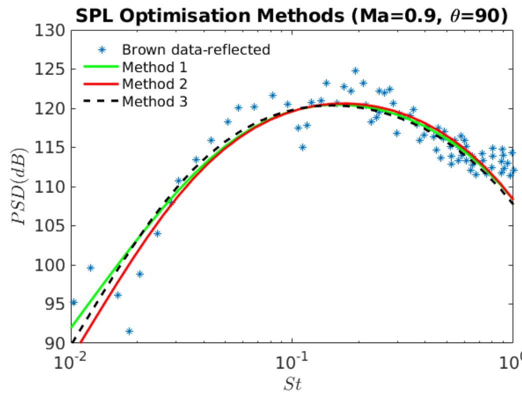

Fig. 1 Ma=0.9, $\theta = 90$: Acoustic predictions for methods 1,2 and 3

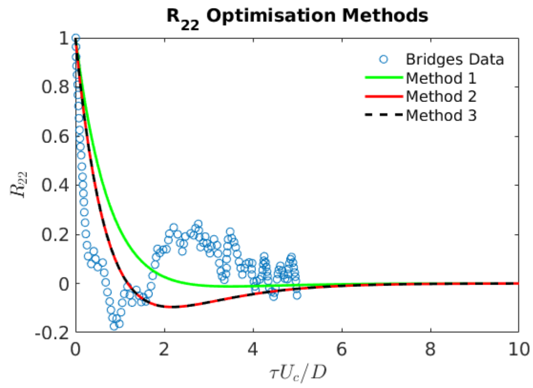

Fig. 2 Turbulence correlation function R_{22} found through Methods 1,2 and 3

4. Concluding Remarks

The *MP-AIDEA* algorithm is effective in optimising the model parameters to give good predictions for the acoustic spectrum for the 3 methods of optimisation. However, to enable a basic representation of the turbulence structure, it is necessary to find the parameter a_1 through the optimisation of the turbulence correlation function before finding the other parameters through optimisation of the acoustic model.

In the talk accompanying this paper, we shall show the acoustic predictions for other acoustic Mach numbers ($Ma = 0.5, 0.7$) and far-field angles ($\theta = 60, 75$), and discuss the optimisation to find one set of parameters for the three acoustic Mach numbers and three far-field angles, with the exception of l_2 which varies with Mach number.

References

[1] M. Goldstein, S. Leib and M. Afsar, *J. Fluid Mech.* 881, (2019), 551–584.

[2] M. Afsar, S. Leib and R. Bozak, *J. Sound and Vib.* 386, (2017), 177–207.

[3] M. Di Carlo, M. Vasile and E. Minisci, *Soft Computing* 24, (2020), 3861–3891.

[4] J. Bridges, *12th AIAA/CEAS Aeroacoustics Conference* AIAA-2006-2534, (2006).